

# Pumped Hydro Storage Balancing in Decarbonization Scenarios, and Impacts of Renewable Generation Variability

Petry Kristine Nøttum Haaland, Erik Seeger Bjørnerem, Magnus Korpås, Ole-Morten Midtgård  
 Department of Electric Energy, Norwegian University of Science and Technology (NTNU), O. S. Bragstads Plass  
 2E, 7034 , Trondheim, Norway  
[petry.k.n.haaland@ntnu.no](mailto:petry.k.n.haaland@ntnu.no)

**Abstract**—To achieve future climate goals, a rapid transition towards a decarbonized power system is essential. This study investigates the impact of pumped hydro storage (PHS) as a form of seasonal storage, within a simplified North European energy system for 2040. Utilizing the capacity expansion model GenX, we explore how uncertainty in variable renewable energy (VRE) profiles influences optimal investment decisions. Our results indicate significant variations in optimal investment decisions based on different weather profiles. Consequently, excluding uncertainty in weather profiles during the planning phase may lead to suboptimal system operation, with unexpectedly high electricity prices. Additionally, we find that PHS can mitigate some of these effects, particularly in the most extreme scenarios.

**Index Terms**—Seasonal storage, Pumped Hydro Storage, Capacity Expansion, RES.

## I. INTRODUCTION

The promotion of renewable energy is widely regarded as a key strategy for achieving a climate-neutral economy [1]. Given that the electricity and heating sectors currently contribute approximately 30% of global emissions, integrating renewable energy sources (RES) has significant potential to reduce these emissions [2].

Numerous studies have demonstrated the feasibility of a 100% renewable energy system [3], [4], [5]. However, a critical challenge for systems with a high share of RES lies in the intermittent nature of wind and solar power. To ensure reliable electricity supply, energy storage solutions are essential [6], [7], [8], [9]. Research further indicates that incorporating storage can reduce overall system costs by enabling the system to better utilize intermittent energy during deficit periods, while minimizing curtailment of excess renewable energy [6], [9].

Renewable energy systems are characterized not only by daily fluctuations but also seasonal variations, necessitating storage solutions with longer durations. Recent years have seen increasing attention to the sizing and duration of energy storage [10], [11], [12], [13], [14]. Studies show that the introduction of long-duration storage reduces system costs in power systems with a high share of solar and wind energy, substantially lowering the required capacities of these sources while ensuring power reliability [10], [15]. Among potential

storage solutions, pumped hydro storage (PHS) has been highlighted as a promising option for balancing intermittent renewable energy generation with long-term storage needs [10], [16].

In Norway, there is considerable potential for PHS, with an existing storage capacity of 85 TWh in Norwegian hydropower reservoirs [17]. Upgrading existing hydropower plants requires significant investment, but could be profitable while ensuring secure access to power [17], [18], [19]. Additionally, utilizing existing reservoirs minimizes environmental impacts by reducing the need for extensive infrastructure developments that could harm untouched natural areas and biodiversity [17], [18], [19], [20].

As previously noted, several studies have concluded that low-emission power systems are feasible. However, many of these studies rely on a single year of weather data, which poses challenges due to the significant year-to-year variability in variable renewable energy (VRE) patterns. This variability is expected to increase due to climate change [1], and using only one year of data may lead to inefficiencies and suboptimal system operation [15].

In [15], the authors analyzed the impacts of interannual variability and energy storage systems (EES) on the hourly profiles of VRE sources. Their findings suggest that investments in EES reduce overall system costs. However, the study has not fully examined the role of seasonal energy storage in this context. In [10], the authors found that the reliance on long-duration storage increased when optimizing power systems over multiple years instead of a single year.

Building on previous research, this study analyzes the impact of PHS as a form of seasonal storage, along with the effects of interannual variability in hourly VRE profiles in a North European energy system for 2040. This study seeks to address the following research questions: What role does PHS play in a power system dominated by VREs, and how does uncertainty in VRE profiles impact optimal operation and investment decisions?

The primary contribution of this study is an evaluation of a decarbonization pathway for Northern Europe by 2040, focusing on the role of PHS as seasonal storage in a power system with a high share of VREs. Additionally, we assess the impacts of uncertainty in VRE profiles on investment decisions and optimal system operation. The rest of this paper is organized

as the following: Section II outlines the methodology and Section III presents input data and assumptions. Section IV presents the results and offers a discussion of the findings. Lastly, Section V gives concluding remarks.

## II. MODELING FRAMEWORK

The modeling framework is based on the open-source electricity resource capacity expansion model GenX [21]. It is a constrained linear or mixed-integer linear optimization model determining the investment portfolio and operational decisions for electricity generation, transmission, storage, and demand-side resources to meet a future electricity demand [21]. GenX is developed in Julia using the JuMP optimization package, and employs minimum-cost planning to identify the necessary investments while adhering to various power system operational constraints, resource availability limits, and other market design, environmental, or policy constraints [21]. The model is deterministic and typically solves a capacity expansion problem for a future year, using the following objective function:

$$\begin{aligned}
\min \quad & \sum_{z \in Z} \sum_{g \in G} (C_{g,z}^{\text{Inv}} \cdot A_{g,z} \cdot \delta_{g,z}^{\text{Inv}} + C_{g,z}^{\text{FixOM}} \cdot \Delta_{g,z}) \\
& + \sum_{z \in Z} \sum_{t \in T} \sum_{g \in G} (C_{g,z}^{\text{VarOM}} + C_{g,z}^{\text{Fuel}}) \cdot \phi_{g,t,z} \\
& + \sum_{z \in Z} \sum_{t \in T} (C_s^{\text{VarOM}} \cdot \phi_{s,t,z} + C_s^{\text{VarOM}} \cdot \phi_{s,t,z}) \\
& + \sum_{z \in Z} \sum_{t \in T} (C^{\text{curt}} \cdot \gamma_{t,z}^e + C^R \cdot \gamma_{t,z}^r) \\
& + \sum_{z \in Z} \sum_{t \in T} \sum_{g \in G} (\Pi_{g,z}^{\text{START}} + \epsilon_{g,t}) \\
& + \sum_{l \in L} \pi_l^{\text{TCAP}} \cdot \Delta \phi_l^{\text{max}} \quad (1)
\end{aligned}$$

The first summation manages the fixed cost, and the second term corresponds to the variable operation and maintenance (O&M) costs. The third summation presents the variable O&M costs of storage, charging and discharging. In the fourth term, penalties for demand curtailment and unmet reserves are added to the objective, whereas the fifth term represents the startup costs for technologies using unit commitment decisions. The last summation accounts for the costs associated with network reinforcement or construction for transmission lines and distribution zones.

The model further works under several technology-specific constraints. Operational limits as startup costs and upper and lower generation limits, resource availability, and cycling of storage technologies can for instance be included for the different technologies [21]. There also exists constraints regarding unit commitment, reserves, and regulation of individual technologies. Additionally, the model regards constraints on system-level, including hourly energy balance, energy transport constraints between areas, total reserve requirements and constraints for total CO<sub>2</sub> emissions [21]. For more detailed information, the reader is referred to [21].

Initial testing showed extreme utilization of the hydropower reservoirs. Due to environmental restrictions, this is unwanted,

and equation 2 was added to avoid draining the hydropower reservoirs below 25% for any time step  $t$ , for all plants  $y$  and all zones  $z$ .

$$\Gamma_{y,z,t} \geq 0.25 \Gamma_{y,z}^{\text{MAX}} \quad \forall y \in Y, z \in Z, t \in T \quad (2)$$

As GenX only models electricity, the conversion from water to electricity is simplified, not accounting for losses due to varying efficiency of hydropower turbines and generators. PHS plants are modeled as batteries separate from the existing hydropower reservoirs, leading to inaccurate storage handling. These are simplifications that overestimate the flexibility potential from PHS but should not largely impact the results on an aggregated scale.

## III. NORTHERN EUROPEAN CASE STUDY

To examine the impact of uncertainty in generation variability, a case study of a simplified North-European power system is conducted. The analysis utilizes the GenX modeling framework, which has been adapted for this purpose.

### A. System description

The studied system consists of three interconnected regions, each connected by transmission lines. Area 1 is predominantly powered by renewable energy sources, including solar, wind and hydropower, representing a simplified version of the Norwegian and Swedish energy systems. In contrast, Areas 2 and 3 primarily rely on thermal energy sources such as gas, coal, and nuclear power, supplemented by some renewable energy production. Area 2 corresponds to Denmark, Germany, Belgium, and the Netherlands, while Area 3 corresponds to the United Kingdom. The selection of these areas reflects the distinct energy mixes within each region. Area 1, with its heavy reliance on renewable energy, has relatively low total emissions, while Areas 2 and 3 show higher annual emissions due to their greater dependence on thermal energy generation. Furthermore, the Netherlands frequently faces a power deficit, requiring significant power imports, whereas Norway typically maintains a power surplus, leading to power exports. This configuration offers a representative model of diverse energy sources and consumption patterns, capturing the complexity of energy generation and trade within the region.

A brownfield optimization approach is adopted, maintaining current capacities as reported by ENTSO-E [22], as shown in Table V in the appendix. We have simplified the assessment to limit VRE sources and natural gas, thus no additional expansion of nuclear power, conventional hydropower, or run-of-river projects is permitted.

Hydropower operations are optimized over a one-year horizon, accounting for historical inflow data, reservoir capacities, power-to-energy ratios, and minimum reservoir thresholds. Inflow data is sourced from [23], featuring different profiles for the different areas, accounting for later snow-melt in Norway and Sweden. For run-of-river, the same inflow values are used, given the lack of hourly data. However, this simplification is expected to have a minimal impact on results, due to the relatively small existing capacity of run-of-river plants

in the dataset. PHS can only invest in pump capacity and not reservoir capacity. Existing reservoirs with PHS potential are collected from [24] (Table 11, 10km, Realizable potential). In addition to PHS, we consider lithium-ion batteries technologies with 4 hours duration. Cost assumptions for batteries are sourced from [25] and listed in appendix, Table VIII. Cost projections are based on the moderate scenario for NREL’s utility-scale battery storage projections for 4-hour duration lithium-ion batteries [25]. Storage costs are found by multiplying the costs in \$/kW with the duration of the battery [26].

Fuel prices and CO<sub>2</sub> emissions factors for each generating unit are detailed in the appendix (Table VI), with fuel prices based on [27] and CO<sub>2</sub> content derived from [28]. To enhance computational efficiency, power plants are grouped into clusters, with each plant within a cluster exhibiting homogeneous characteristics. Bioenergy production is assumed to be emission-free, following [29]. Generation unit parameters for capacity expansion are presented in Table VII in the appendix. Hourly availability factors for RES are obtained from [30], with inter-annual variability captured through capacity factors from 2007 to 2019. Nuclear power’s hourly availability data, including annual scheduled maintenance, is sourced from [23], while constant availability factors are assumed for all other generation technologies. Investment costs, as well as fixed and variable O&M expenses, are shown in Table VIII in appendix and are based on the EU Reference Scenario 2020 [31]. A discount rate of 5% is applied to calculate annuity costs across all technologies. Table IX in the appendix provides transmission capacities between zones, aggregated from existing infrastructure data as specified in the ENTSOG and ENTSO-E’s Ten-Year Network Development Plans (TYNDPs), with a 3% loss factor assumed for HVDC links. Hourly demand variations are based on historical average data from 2015–2021 collected from [22], and adjusted upwards according to forecasts from [27]. The demand growth assumptions include a 20% increase by 2030 from current levels, as per [32], followed by a 25% increase relative to levels of 2030 by 2040 [27]. The value of lost load (VoLL) is set to \$10,000/MWh.

### B. Description of scenarios

To investigate the impacts of uncertainty in VRE profiles on investment decisions and optimal system operation, three distinct cases (hereafter referred to as cases 1, 2, and 3) are analyzed. These cases employ varying solar, wind, and inflow profiles, as outlined in Table I.

- Case 1: Represents a dry historical year characterized by low inflow and favorable solar conditions, found to be 1996.
- Case 2: Reflects average inflow and VRE profiles. The VRE profiles are taken from the median year derived from historical data spanning 2007–2019, found to be 2013.
- Case 3: Represents a historical year with high inflow and unfavorable solar conditions, found to be 2000.

The cases are designed to assess how uncertainty in VRE profiles affects final investment decisions in the GenX model.

TABLE I: Weather year assumptions for specified case studies. I is the inflow profile for case 2.

Parameter	Case 1	Case 2	Case 3
Inflow profile	0.75 · I <sub>avg</sub>	I <sub>avg</sub> <sup>1</sup>	1.26 · I <sub>avg</sub>
Solar and wind profile	1996	2013	2000

<sup>1</sup>Inflow profile, collected from [23].

The solar and wind profiles for cases 1 and 3 are chosen based on analyzing historical capacity factors for solar and wind, together with historical inflow series from 1990 until today. The annual capacity factors (CFs) can be seen in Table II. For hydropower inflow, the same profiles are used for cases 1 and 3, but they are scaled to account for changes in total annual inflow, based on historical data for years 1996 and 2000. The two years were chosen based on analyzing historical inflow profiles for 1990 until today, representing years with low and high inflow, respectively.

TABLE II: Annual capacity factors for specified case studies [solar, onshore wind, offshore wind].

Zone	Case 1	Case 2	Case 3
1	[0.10, 0.24, 0.49]	[0.10, 0.25, 0.46]	[0.09, 0.28, 0.51]
2	[0.13, 0.22, 0.32]	[0.12, 0.22, 0.32]	[0.12, 0.25, 0.36]
3	[0.11, 0.29, 0.38]	[0.11, 0.30, 0.38]	[0.11, 0.29, 0.39]

The initial cases are conducted by imposing a CO<sub>2</sub> cap set at 90% of 1990 emission levels, in alignment with the objectives of the European Union outlined in [33]. The simulations are then repeated, allowing the model to invest in PHS to assess the impact of long-duration storage on investment decisions.

### C. Cross-application of scenarios

Uncertainties in weather data may impact the optimal investment decisions of the system. To examine this effect more closely, we conduct simulations by cross-applying the optimal installed capacity from one case to the other cases, as shown in Table III.

TABLE III: Cross-application of scenarios.

Weather profile	Installed capacity		
	Case 1 capacity	Case 2 capacity	Case 3 capacity
Case 1		x	x
Case 2	x		x
Case 3	x	x	

## IV. RESULTS AND DISCUSSION

This section presents the results from the three cases outlined in Section III-B, focusing on the impact of long-duration storage and the year-to-year VRE profiles.

### A. Power System Configuration and Impact of Pumped Hydro Storage Installation

Originally, all cases involve significant investments in RES, driven by the low investment costs projected for renewable

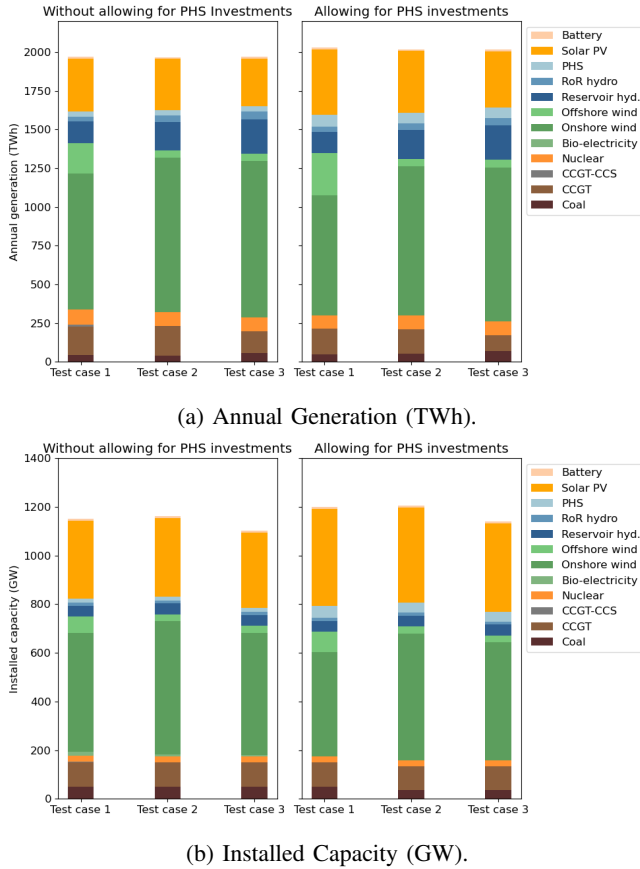


Fig. 1: (a) Annual generation (TWh) and (b) installed capacity (GW) for test cases 1, 2, and 3 under a 90% CO<sub>2</sub> emission reduction target, with and without PHS investment options.

energy in 2040, as seen in Fig. 1. The system also has the option to invest in short-duration batteries (4-hour storage). However, due to the high investment cost associated with this technology, no investment is done in new short-duration battery capacity. As seen from Fig. 1b, cases 1 and 2 install the highest share of VRE capacity. Despite this, case 3 achieves almost the same amount of VRE generation, due to better wind conditions and higher inflow profiles, as seen in Fig. 1a. VRE power production accounts for 72%, 70%, and 69% of total generation for cases 1, 2 and 3, respectively. Case 1 achieves the highest share of VRE generation, due to a large investment in offshore wind power. As illustrated in Fig. 1a, onshore wind capacity is most favored across all scenarios, and the share of onshore wind power is 45%, 51%, and 51% for cases 1, 2, and 3, respectively.

Allowing for PHS investments results in a further increase in VRE capacity. The installed PHS facilitates more PV capacity, as it becomes possible to store excess PV production for later periods. Onshore wind capacity decreases compared to the scenario without PHS investment, now contributing 38%, 48% and 49% of total production, which can be attributed to higher costs relative to PV. However, onshore wind capacity remains dominant. PHS capacity is relatively similar across all cases, though it is higher in case 1, which has greater PV investments due to better PV conditions and poorer wind conditions. VRE

power production now accounts for 72%, 70%, and 70% of total generation, which is almost equal to the scenario without PHS investments. Again, case 1 has the highest share of VRE production due to even larger investments in offshore wind compared to the scenario without PHS. However, as seen in Fig. 1a, the amount of VRE production is relatively similar across the different cases.

As mentioned, onshore wind production dominates across all scenarios, with some variation based on the chosen input profile. The variation in wind production is strongly associated with the annual CFs, as presented in Table II, thus indicating relying on a single weather year can result in suboptimal operation in other years, aligning with the findings in [15]. However, the observed annual variation in CFs is modest, leading to only minor differences in wind production. Permitting PHS investments leads to a greater variation in onshore wind production across different scenarios. This is mainly due to the inflow profiles, which significantly influence changes in power production.

Fig. 2 shows the operation of PHS in areas 1 and 2 for case 2. In Fig. 2b, Area 2 features daily balancing with pumping during the middle of the day and discharge during both morning and evening peaks. This is different from traditional scheduling, where the pumps are run during the night to avoid ramping down nuclear power plants. Pumping operation is highly correlated with PV availability, providing more discharge during the summer months. During winter, pumping occurs during favorable wind conditions, but due to the lower reservoir size, the PHS still features daily balancing.

The daily balancing pattern is also present for Area 1, but only from April to October (Fig. 2a). This is due to less favorable PV resource availability in this area. Due to a larger storage volume, discharge in Area 1 targets fewer hours during morning and evening peaks, with larger discharge utilization in these hours. This differs from Area 2, which can refill the

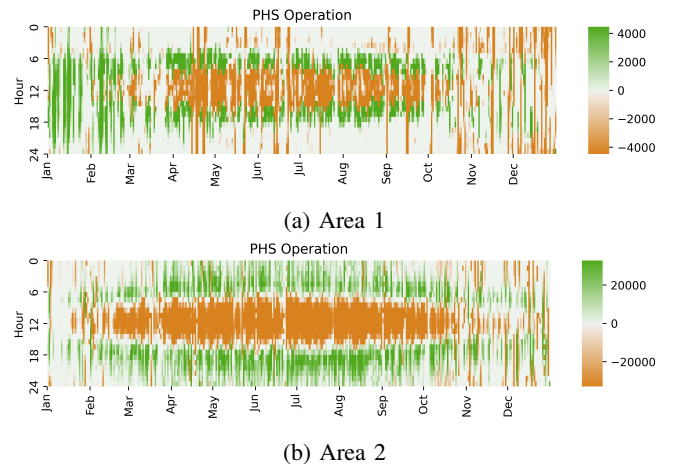


Fig. 2: Pumped hydropower storage operation for case 2, Area 1 (upper) and Area 2 (lower). Discharge is positive (Green) and pumping is negative (Yellow) in MW. Area 1 has a larger reservoir capacity in TWh, but smaller installed pump capacity in MW, compared to Area 2.

PHS daily. In contrast, Area 1 includes long-term storage, with pumping occurring from October to December and discharging from January to March. Additionally, the larger PHS reservoir in Area 1 is able to capture periods with high wind generation, showing multiple days of constant pumping throughout the year. This is shown as solid vertical lines in Fig. 2a.

### B. Simulating Interactions Between Optimal Scenarios for Performance Analysis

In this section the most noteworthy results from cross-applying the different scenarios from Tab III are presented. These were case 1 using the installed capacity of case 3, case 2 using the installed capacity of case 3, and case 3 using the installed capacity of case 1.

1) *Electricity prices:* Simulating interactions between optimal scenarios have a substantial impact on electricity prices, with the most pronounced effect observed in case 1. In the GenX framework, electricity prices are reported as the marginal electricity price for each area and time step [21], corresponding to the dual variable of the power balance constraint. Table IV summarizes the average annual electricity prices for each zone. Price duration curves can be seen in Appendix C.

As shown in Table IV, simulating case 1 with the installed capacity of case 3 results in exceptionally high electricity prices, caused by an energy deficit due to lower VRE availability. This is expected as deterministic planning for a single weather-year does not leave any slack accounting for variations in inflow and VRE availability. Additionally, the strict CO<sub>2</sub>-restriction limits how much of the energy deficit may be covered by thermal generation, thus leading to marginal prices often being set by the VoLL or carbon free technologies such as nuclear or bio. In this simulation, nuclear is already maxed out, and bio sets the marginal price at 719 \$/MWh for the majority of the year (see Fig 4). However, the observed electricity prices are significantly lower for case 1 if the original case 3 investment were made including PHS upgrades. With additional PHS capacity, load-shedding is reduced by 146 GWh (42%), thus reducing the number of hours where the VoLL sets the electricity price. The prices are still around double the price level in the original case 1 solution, but they seem more realistic compared to the impact of a dry weather year. Even though these results are derived from a single weather year, they showcase benefits from having additional flexibility from PHS capacity, which is able to utilize more of the available VRE generation, by reducing energy deficits through temporal shifting.

Electricity prices also rise for case 2 when using the optimal decision for case 3, although not to the same extent as for case 1. Again, the introduction of PHS reduces electricity prices. However, this case features more inflow, making the system less affected by the cross-application. For case 3, a different outcome is observed when using the optimal capacities from case 1. In this scenario, electricity prices drop significantly in Area 1 compared to the original solution from case 3. Prices also decrease in Areas 2 and 3, albeit not as dramatically. Due to higher inflow, case 3 initially installs less VRE capacity

compared to case 1. Consequently, excess VRE generation leads to an energy surplus and more zero-price hours. This is also reflected in VRE curtailment, which increases from 8.81% to 16.95% of total power generation. For this simulation, there is little impact of PHS in the original investment decision. For all scenarios, Area 3 is little impacted due to limited transmission capacity from the other areas.

TABLE IV: Resulting average annual area prices (\$/MWh) from running simulations using optimal investment capacity from each other case [Area 1, Area 2, Area 3].

Cross-appli. of optimal capacities	Case 1 (using Case 3 capacity)	Case 2 (using Case 3 capacity)	Case 3 (using Case 1 capacity)
Original sol., for comp. (No PHS)	[42.8, 60.9, 49.6]	[40.6, 40.6, 48.0]	[34.5, 54.1, 50.0]
Cross-appli. (No PHS)	[682.3, 572.0, 76.3]	[67.2, 68.0, 54.0]	[3.5, 49.5, 44.7]
Cross-appli. (With PHS)	[108.9, 107.2, 64.8]	[65.7, 62.4, 54.2]	[2.6, 48.3, 45.5]

Abbreviations: Sol.: Solution, Comp.: Comparison, Appli.: Application

## V. CONCLUSION

In this study, we have investigated three distinct cases to assess the impact of uncertainty in VRE input profiles, namely case 1 representing a dry year, case 2 representing a median year, and case 3 representing a wet year. Our findings indicate that the utilization of different VRE profiles does not necessarily lead to significant changes in installed capacity or scheduled generation. Conversely, it is inflow that plays a larger role in influencing generation, which is reasonable when one area has a large share of existing hydropower capacity. This is further evidenced when applying the optimal decisions from one case to another. For instance, using the optimal decision from case 3, characterized by high inflow, on case 1, with low inflow, leads to exceedingly high electricity prices due to high rationing. Conversely, applying the optimal decision for case 1 to case 3 results in lower electricity prices, due to surplus VRE generation introducing more zero-price hours. This indicates that relying on a single weather year for dimensioning an energy system can result in considerable suboptimal operation in other years, aligning with findings in previous work. This further underscores the importance of incorporating uncertainty in VRE and inflow profiles when planning future power system investments and operation.

This study also explored the role of PHS in a power system dominated by VRE. The findings indicate that permitting PHS investments can significantly reduce electricity prices in extreme cases, as the added flexibility can reduce the risk of rationing. Additionally, increased PHS capacity leads to higher PV capacity, as it becomes profitable to utilize daily balancing due to cheap PV generation. Seasonal balancing is only present in the Nordics, due to the continental PHS reservoir being rather small compared to the demand. Thus, system wide impacts of using PHS for balancing VRE generation are rather small, and could be improved by increased transmission connecting the PHS to surplus VRE generation.

## VI. AI DECLARATION

During the preparation of this work we used Copilot to improve language and to write the initial code for plotting Figs. 1, 3, and 4. After using this tool/service, we reviewed and edited the content as needed and take full responsibility for the content of the publication.

### REFERENCES

- [1] C. et al., “IPCC, 2023: Climate change 2023: Synthesis report. contribution of working groups I, II and III to the sixth assessment report of the intergovernmental panel on climate change [core writing team, H. Lee and J. Romero (eds.)]. IPCC, Geneva, Switzerland.” P. Arias, M. Bustamante, I. Elgizouli, G. Flato, M. Howden, C. Méndez-Vallejo, J. J. Pereira, R. Pichs-Madruga, S. K. Rose, Y. Saheb, R. Sánchez Rodríguez, D. Ürge Versatz, C. Xiao, N. Yassaa, J. Romero, J. Kim, E. F. Haites, Y. Jung, R. Stavins, A. Birt, M. Ha, D. J. A. Orendain, L. Ignon, S. Park, Y. Park, A. Reisinger, D. Cammaramo, A. Fischlin, J. S. Fuglestvedt, G. Hansen, C. Ludden, V. Masson-Delmotte, J. R. Matthews, K. Mintenbeck, A. Pirani, E. Poloczanska, N. Leprince-Ringuet, and C. Péan, Eds. Intergovernmental Panel on Climate Change (IPCC), edition: First. [Online]. Available: <https://www.ipcc.ch/report/ar6/syr/>
- [2] 4 charts explain greenhouse gas emissions by sector | world resources institute. [Online]. Available: <https://www.wri.org/insights/4-charts-explain-greenhouse-gas-emissions-countries-and-sectors>
- [3] Towards 100 percent renewable energy status trends and lessons learned. [Online]. Available: <https://www.irena.org/publications/2019/Jan/Towards-100-percent-renewable-energy-status-trends-and-lessons-learned>
- [4] C. Breyer, S. Khalili, D. Bogdanov, M. Ram, A. S. Oyewo, A. Aghahosseini, A. Gulagi, A. A. Solomon, D. Keiner, G. Lopez, P. A. Østergaard, H. Lund, B. V. Mathiesen, M. Z. Jacobson, M. Victoria, S. Teske, T. Pregger, V. Fthenakis, M. Rauegi, H. Holttinen, U. Bardi, A. Hoekstra, and B. K. Sovacool, “On the history and future of 100% renewable energy systems research,” vol. 10, pp. 78 176–78 218, conference Name: IEEE Access. [Online]. Available: <https://ieeexplore.ieee.org/document/9837910>
- [5] M. O’Malley, “Editorial: Towards 100% renewable energy system,” vol. 37, no. 4, pp. 3187–3189, conference Name: IEEE Transactions on Power Systems. [Online]. Available: <https://ieeexplore.ieee.org/document/9799720>
- [6] H. Jafarizadeh, E. Yamini, S. Zolfaghari, F. Esmaeilion, M. Assad, and M. Soltani, “Navigating challenges in large-scale renewable energy storage: Barriers, solutions, and innovations,” vol. 12, pp. 2179–2192.
- [7] O. Bamisile, D. Cai, H. Adun, M. Dagbasi, C. C. Ukwuoma, Q. Huang, N. Johnson, and O. Bamisile, “Towards renewables development: Review of optimization techniques for energy storage and hybrid renewable energy systems,” vol. 10, no. 19, p. e37482.
- [8] J. Z. Cui, C. Xie, W. Wu, S. D. Widijatmoko, Y. Hong, Y. Li, and G. A. Leeke, “Techno-economic analysis of deploying a short or mixed energy storage strategy in a 100% green power grid,” vol. 99, p. 113333. [Online]. Available: <https://www.sciencedirect.com/science/article/pii/S2352152X24029190>
- [9] S. Freeman and E. Agar, “The impact of energy storage on the reliability of wind and solar power in new England,” vol. 10, no. 6, p. e27652.
- [10] J. A. Dowling, K. Z. Rinaldi, T. H. Ruggles, S. J. Davis, M. Yuan, F. Tong, N. S. Lewis, and K. Caldeira, “Role of long-duration energy storage in variable renewable electricity systems,” vol. 4, no. 9, pp. 1907–1928. [Online]. Available: <https://www.sciencedirect.com/science/article/pii/S2542435120303251>
- [11] J. A. Dowling and N. S. Lewis, “Long-duration energy storage for reliable renewable electricity: The realistic possibilities,” vol. 77, no. 6, pp. 281–284, publisher: Routledge. eprint: <https://doi.org/10.1080/00963402.2021.1989191>. [Online]. Available: <https://doi.org/10.1080/00963402.2021.1989191>
- [12] S. Ashfaq, I. El Myasse, D. Zhang, A. S. Musleh, B. Liu, A. A. Telba, U. Khaled, and M. Metwally Mahmoud, “Comparing the role of long duration energy storage technologies for zero-carbon electricity systems,” vol. 12, pp. 73 169–73 186, conference Name: IEEE Access. [Online]. Available: <https://ieeexplore.ieee.org/document/10521612>
- [13] J. Twitchell, K. DeSomber, and D. Bhatnagar, “Defining long duration energy storage,” vol. 60, p. 105787. [Online]. Available: <https://www.sciencedirect.com/science/article/pii/S2352152X22017753>
- [14] P. Albertus, J. S. Manser, and S. Litzelman, “Long-duration electricity storage applications, economics, and technologies,” vol. 4, no. 1, pp. 21–32. [Online]. Available: <https://www.sciencedirect.com/science/article/pii/S2542435119305392>
- [15] M. Jafari, M. Korpås, and A. Botterud, “Power system decarbonization: Impacts of energy storage duration and interannual renewables variability,” vol. 156, pp. 1171–1185. [Online]. Available: <https://www.sciencedirect.com/science/article/pii/S0960148120306820>
- [16] P. Nikolaos, F. Marios, and D. Katsaprakakis, “A review of pumped hydro storage systems,” vol. 16, p. 4516.
- [17] M. M. Belsnes. Norwegian pumped storage hydropower could help stabilise electricity prices. [Online]. Available: <https://blog.sintef.com/sintefenergy/norwegian-pumped-storage-hydropower-could-help-stabilise-electricity-prices/>
- [18] L. I. Pitorac, “Upgrading of hydropower plants to pumped storage plants: Tunnel system hydraulics,” accepted: 2021-11-01T07:39:49Z ISBN: 9788232652099 ISSN: 2703-8084. [Online]. Available: <https://ntnuopen.ntnu.no/ntnu-xmlui/handle/11250/2826677>
- [19] hydroreviewcontentdirectors. How pumped storage hydropower could help stabilize Norway’s electricity prices. [Online]. Available: <https://www.hydroreview.com/>

com/hydro-industry-news/pumped-storage-hydro/pumped-storage-hydropower-could-help-stabilize-norways-electricity-prices/

- [20] T. Tellefsen, J. Van Putten, and O. Gjerde, “Norwegian hydropower: Connecting to continental europe,” vol. 18, no. 5, pp. 27–35. [Online]. Available: <https://ieeexplore.ieee.org/document/9171529/>
- [21] J. D. Jenkins and N. A. Sepulveda, “Enhanced decision support for a changing electricity landscape: The GenX configurable electricity resource capacity expansion model,” accepted: 2021-05-13T17:24:21Z. [Online]. Available: <https://dspace.mit.edu/handle/1721.1/130589>
- [22] Power statistics. [Online]. Available: <https://www.entsoe.eu/data/power-stats/>
- [23] M. Korpås and et al., “Tradewind grid modelling and power system data.”
- [24] M. Gimeno-Gutiérrez and R. Lacal-Aránategui, “Assessment of the european potential for pumped hydropower energy storage based on two existing reservoirs,” vol. 75, pp. 856–868. [Online]. Available: <https://www.sciencedirect.com/science/article/pii/S096014811400706X>
- [25] Utility-scale battery storage | electricity | 2022 | ATB | NREL. [Online]. Available: [https://atb.nrel.gov/electricity/2022/utility-scale\\_battery\\_storage](https://atb.nrel.gov/electricity/2022/utility-scale_battery_storage)
- [26] W. Cole and A. Karmakar, “Cost projections for utility-scale battery storage: 2023 update.”
- [27] ENTSO-e and ENTSG TYNDP 2024 draft scenarios report. [Online]. Available: <https://2024.entsoe-tyndp-scenarios.eu/>
- [28] Carbon dioxide emissions factors. [Online]. Available: <https://ourworldindata.org/grapher/carbon-dioxide-emissions-factor>
- [29] M. Karmellos, D. Kopidou, and D. Diakoulaki, “A decomposition analysis of the driving factors of CO<sub>2</sub> (carbon dioxide) emissions from the power sector in the european union countries,” vol. 94, pp. 680–692. [Online]. Available: <https://www.sciencedirect.com/science/article/pii/S0360544215015406>
- [30] Renewables.ninja. [Online]. Available: <https://www.renewables.ninja/>
- [31] EU reference scenario 2020 - european commission. [Online]. Available: [https://energy.ec.europa.eu/data-and-analysis/energy-modelling/eu-reference-scenario-2020\\_en](https://energy.ec.europa.eu/data-and-analysis/energy-modelling/eu-reference-scenario-2020_en)
- [32] ENTSO-E. Major trends reshaping the power sector — ENTSO-e vision on market design and system operation towards 2030. [Online]. Available: <https://vision2030.entsoe.eu/major-trends-reshaping-the-power-sector/>
- [33] 2040 climate target - european commission. [Online]. Available: [https://climate.ec.europa.eu/eu-action/climate-strategies-targets/2040-climate-target\\_en](https://climate.ec.europa.eu/eu-action/climate-strategies-targets/2040-climate-target_en)

## APPENDIX

### A. Nomenclature

#### Sets

- $g \in G$  Index and set of generators  $g$   
 $l \in L$  Index and set of lines  $l$   
 $t \in T$  Index and set of time periods  $t$   
 $z \in Z$  Index and set of zones  $z$

#### Other Symbols

- $I_{avg}$  Inflow profile for case 2

#### Parameters

- $\Delta\phi_l^{max}$  Maximum power flow on line  $l$   
 $\Delta_{g,z}$  Capacity addition for generator  $g$  in zone  $z$   
 $\delta_{g,z}^{Inv}$  Binary investment decision for generator  $g$  in zone  $z$   
 $\epsilon_{g,t}$  Start-up decision variable for generator  $g$  at time  $t$   
 $\gamma_{t,z}^e$  Curtailment at time  $t$  in zone  $z$   
 $\gamma_{t,z}^r$  Reserve at time  $t$  in zone  $z$   
 $\Gamma_{y,z,t}$  Storage level of storage  $y$  in zone  $z$  for timestep  $t$   
 $\Gamma_{y,z}^{MAX}$  Maximum storage level of storage  $y$  in zone  $z$   
 $\phi_{g,t,z}$  Power output of generator  $g$  in zone  $z$  at time  $t$   
 $\phi_{s,t,z}$  Power output of storage  $s$  in zone  $z$  at time  $t$   
 $\Pi_{g,z}^{START}$  Start-up cost for generator  $g$  in zone  $z$   
 $\pi_l^{CAP}$  Transmission capacity cost for line  $l$   
 $A_{g,z}$  Capacity of generator  $g$  in zone  $z$   
 $C^R$  Cost of reserve  
 $C_{curt}$  Cost of curtailment  
 $C_{g,z}^{FixOM}$  Fixed O&M cost for generator  $g$  in zone  $z$   
 $C_{g,z}^{Fuel}$  Fuel cost for generator  $g$  in zone  $z$   
 $C_{g,z}^{Inv}$  Investment cost for generator  $g$  in zone  $z$   
 $C_{g,z}^{VarOM}$  Variable O&M cost for generator  $g$  in zone  $z$   
 $C_s^{VarOM}$  Variable O&M cost for storage

### B. Input data

This section summarizes the key assumptions underlying this study. It encompasses existing capacity levels (Table V, [22]), fuel prices and associated CO<sub>2</sub> content (Table VI, [27], [28]), characteristics of each generating unit (Table VII, [21]), investment requirements, fixed costs, and O&M expenses (Table VIII, [25], [31]), and transmission capacities between zones (Table IX, [27]).

TABLE V: Existing installed capacity

Generation unit	Area 1 [MW]	Area 2 [MW]	Area 3 [MW]
STHC	0	25155	5755
STLC	0	18949	0
CCGT	459	58715	41371
CCGT CCS	0	0	0
Bio-energy	0	11366	4528
Nuclear	6900	9479	8256
Wind onshore	19830	71544	13932
Wind offshore	0	15917	12160
Solar PV	3200	94452	13470
Run-of-River	6702	3943	1919
Conv. Hydro	43001	1433	0
PHS	1065	10588	4309
Battery 4h	0	3900	3600

Abbreviations: STHC: Steam Turbine Hard Coal,  
 STLC: Steam Turbine Lignite Coal,  
 CCGT: Combined Cycle Gas Turbine,  
 CCS: Carbon Capture and Storage,  
 Conv: Conventional,  
 PHS: Pumped Hydro Storage

TABLE VI: Fuel price and CO<sub>2</sub> content

Fuel	Price (\$/MMBtu)	CO <sub>2</sub> content (tons/MMBtu)
Hard Coal	3.24	0.24
Lignite	3.20	0.28
Natural Gas	8.40	0.10
Nuclear	3.89	0.00
Bio-fuel	48.91	0.00

TABLE VII: Technology efficiency and fuel content

Unit	Type	Efficiency	Fuel
STHC	Thermal	0.43	Coal
STLC	Thermal	0.43	Coal
CCGT	Thermal	0.59	Gas
CCGT CCS	Thermal	0.48	Gas
Bio-energy	Thermal	0.32	Bio-fuel
Nuclear	Thermal	0.38	-
Wind onshore	VRE	NA	-
Wind offshore	VRE	NA	-
Solar PV	VRE	NA	-
Run-of-River	VRE	NA	-
Conventional hydro	Hydro	NA	-
Pumped hydro storage	Storage	0.87	-
Battery 4h	Storage	0.92	-

TABLE VIII: Costs

Generation unit	Investment (\$/MW-year)	Fixed O&M (\$/MW-year)	Variable O&M (\$/MWh)
STHC	112140.36	1979.86	2.62
STLC	131474.90	2513.49	3.27
CCGT	41221.25	1546.76	2.52
CCGT CCS	116007.27	2706.84	3.14
Bio-energy	255602.68	4872.31	6.34
Nuclear	464029.07	8352.52	8.28
Wind onshore	73471.27	928.06	0.20
Wind offshore	140755.48	2242.81	0.43
Solar PV	27300.38	734.71	0.00
Run-of-River	190933.06	9480.00	0.00
Hydropower	249043.13	29840.00	0.37
PHS	290550.31	35100.00	0.00
Battery 4h	66681.12	20166.00	0.00

TABLE IX: Transmission capacities

Line from	Line to	Capacity (MW)
Area 1	Area 2	6975
Area 2	Area 3	4800
Area 1	Area 3	2800

### C. Price duration curve

As seen in Figure 3, not allowing for PHS investments results in more hours with non-served energy, resulting in rationing setting the price. Furthermore, as seen in Figure 4, electricity prices are in general higher, without allowing PHS investments, as more thermal power production is needed to cover for hours with sufficient VRES production. Allowing for PHS investments enables the system to store excess VRES power, again resulting in lower electricity prices.

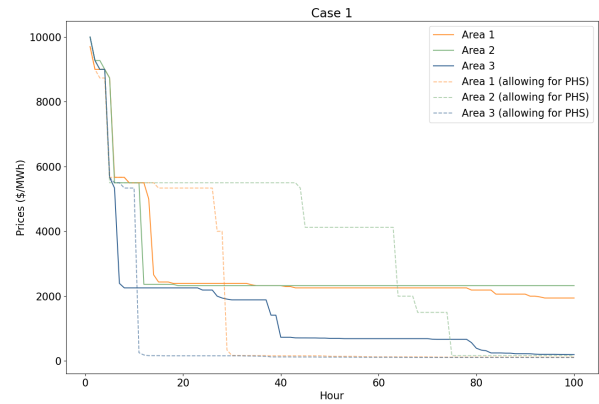


Fig. 3: Price duration curve for case 1 using the optimal capacity of case 3, for the first 100 hours.

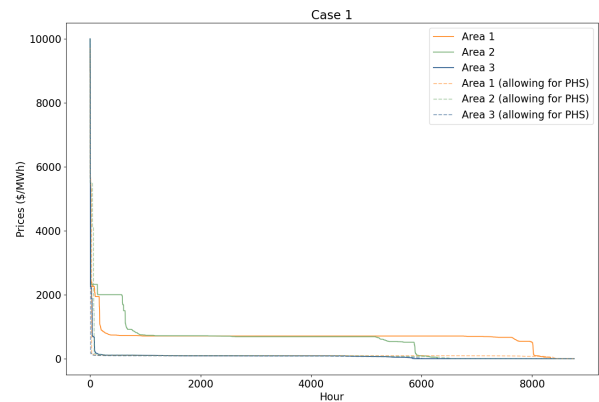


Fig. 4: Price duration curve for case 1 using the optimal capacity of case 3.